Electronic Supplementary Information (ESI)

CrystEngComm

Luminescent Spherical Particles of Lanthanide-based Infinite Coordination Polymers with Tailorable Sizes

Guilherme Arroyos*, Regina Célia Galvão Frem

São Paulo State University (UNESP), Institute of Chemistry, Araraquara, São Paulo, 14800-060, Brazil.

E-mail: guiarroyos@gmail.com

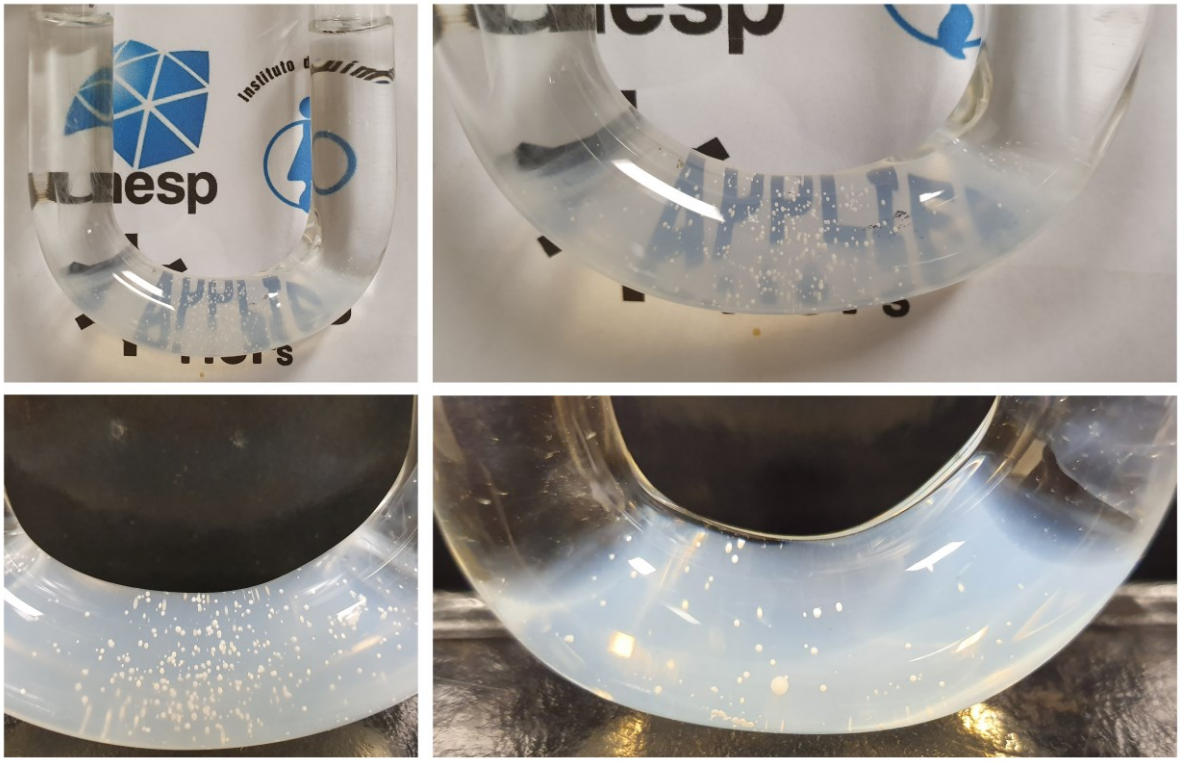

Fig. S1. Photographs of the U-shaped tube + agarose gel system, showing the particles of **Eu-Dif** (top) and **Tb-Dif** (bottom) samples formed in the gel.

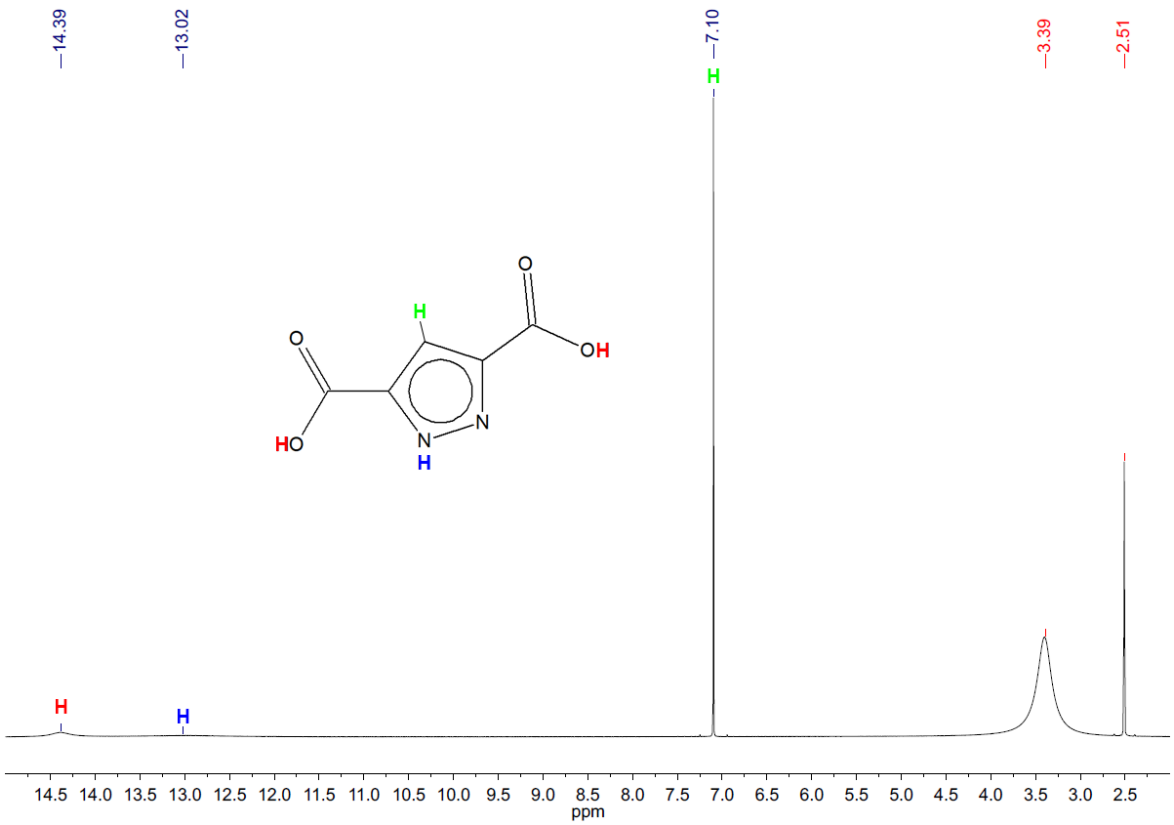

Fig. S2. ^{1}H NMR spectrum of pyrazole-3,5-dicarboxylic acid in DMSO-d6.

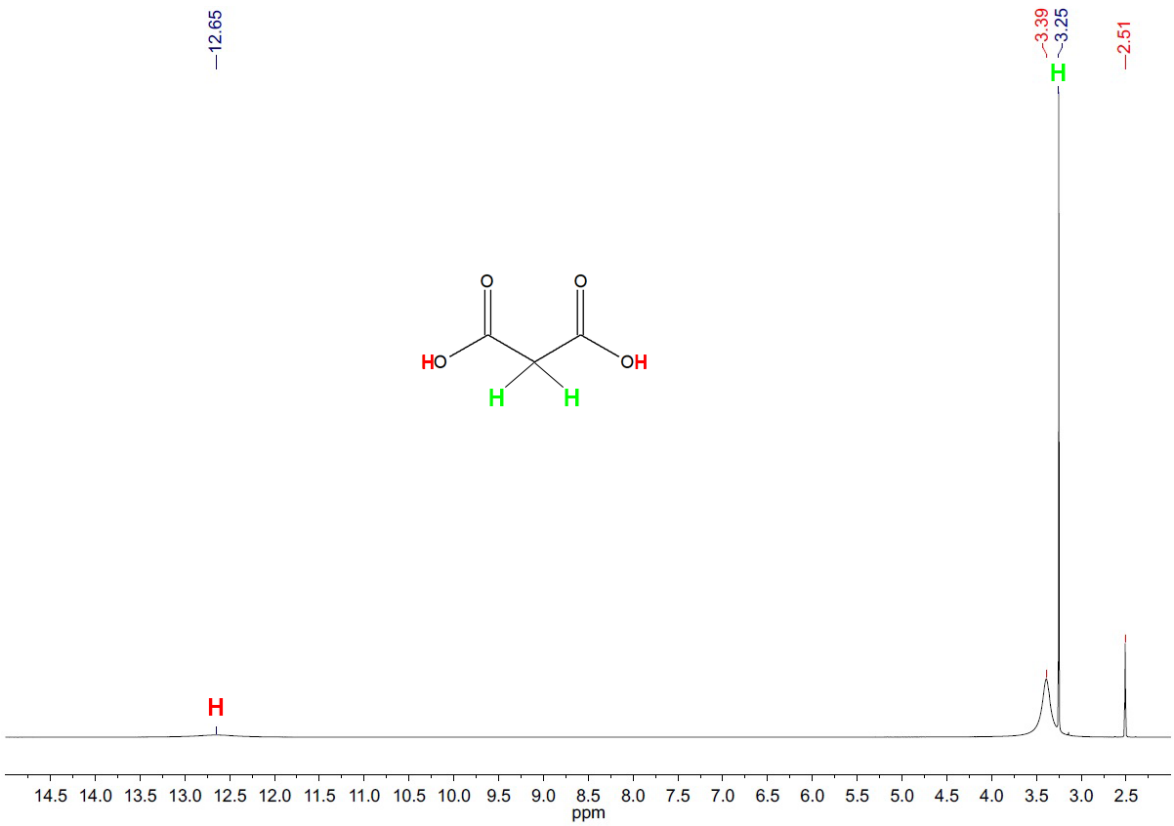

Fig. S3. ^{1}H NMR spectrum of malonic acid in DMSO-d6.

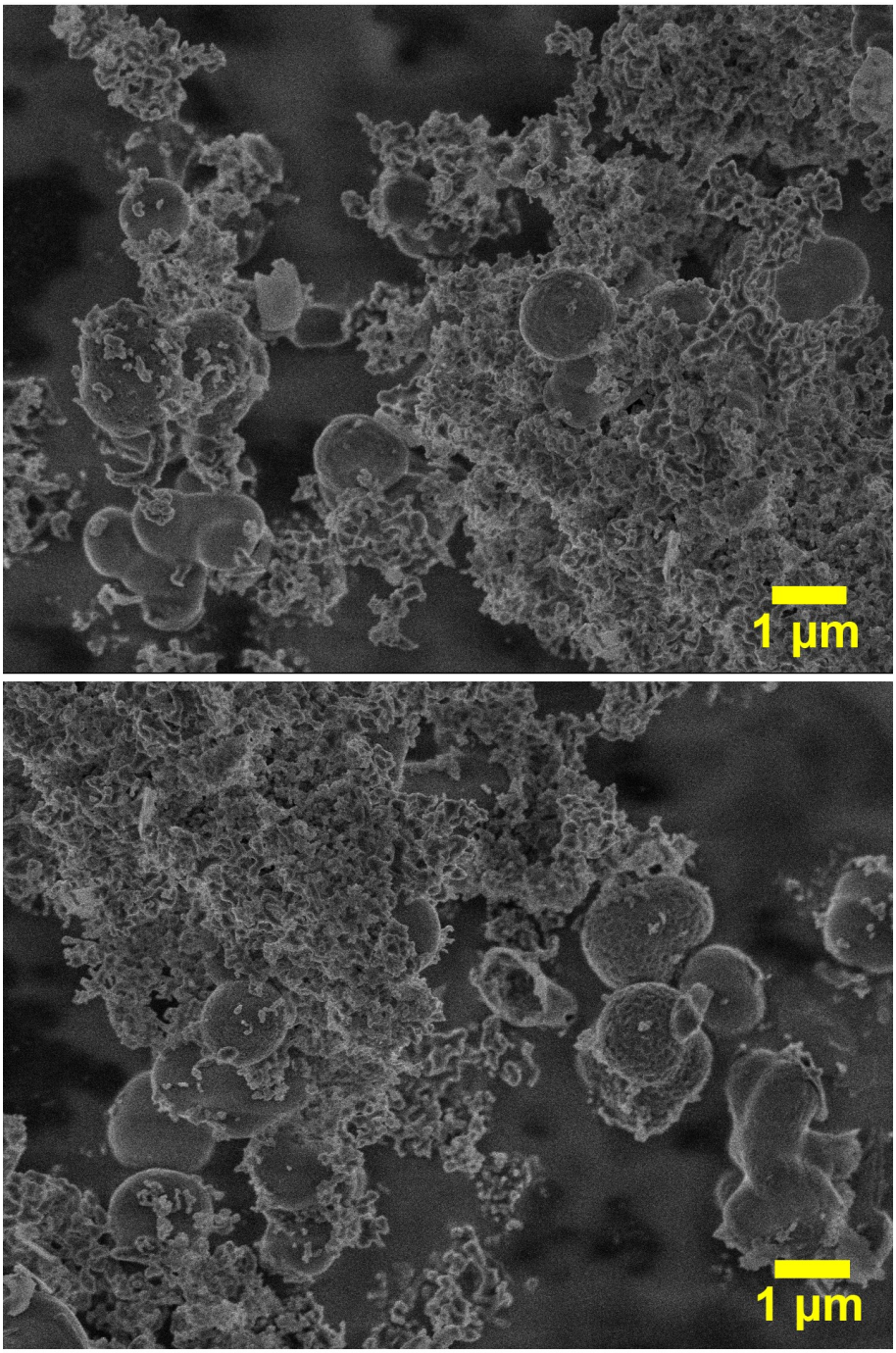

Fig. S4. SEM micrographs of **Tb-M** synthesized without the addition of malonic acid, at pH=4.0.

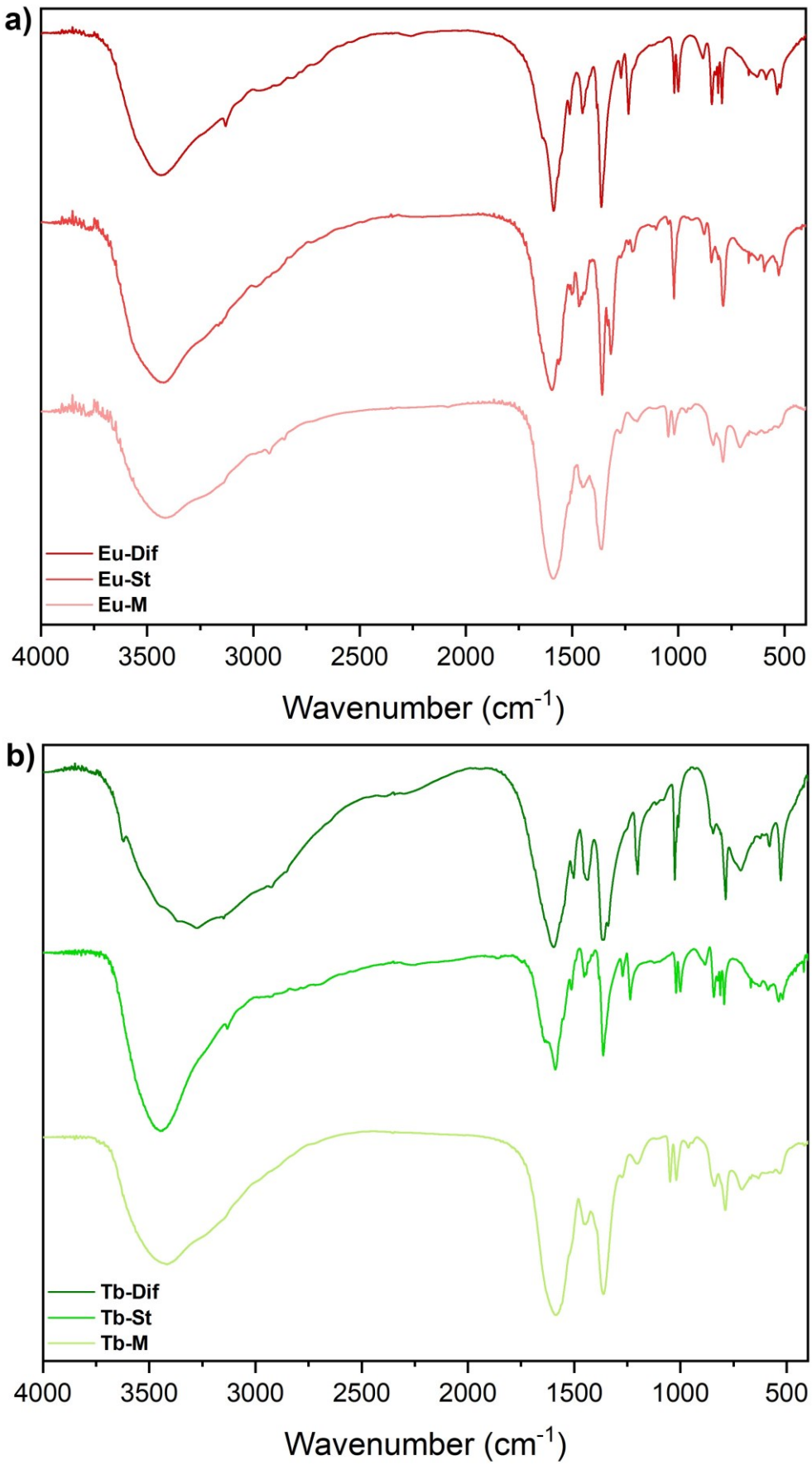

Fig. S5. FTIR spectra of Eu^{3+}-(a) and Tb^{3+}-based (b) samples.

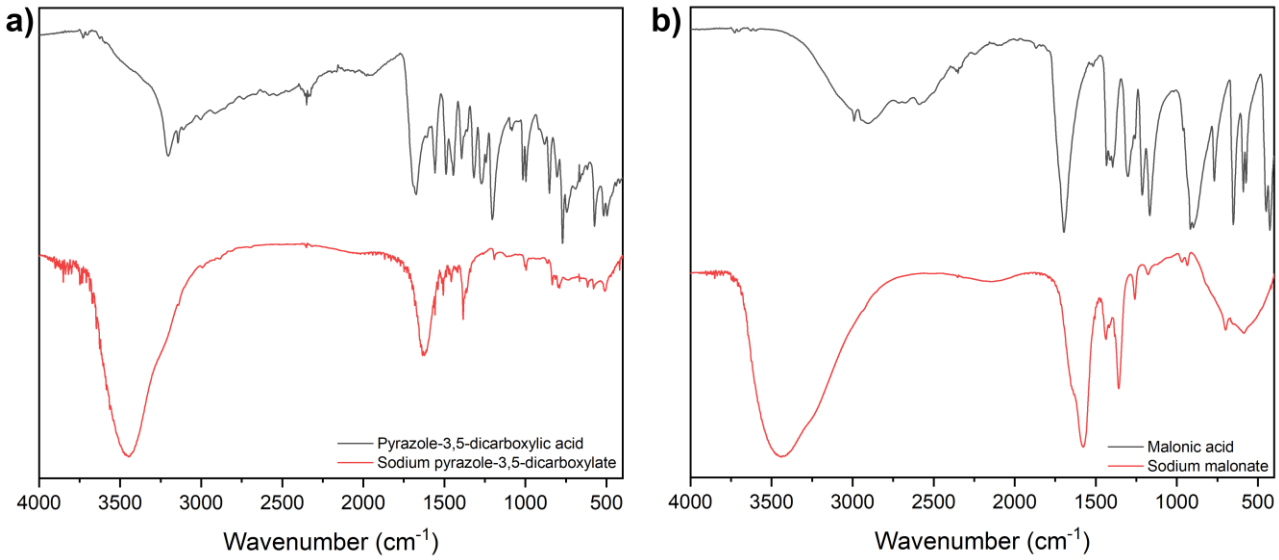

Fig. S6. FTIR spectra of the ligands. a) pyrazole-3,5-dicarboxylic acid (black) and the corresponding sodium salt (red); b) malonic acid (black) and the corresponding sodium salt (red).

In the FTIR spectra (Fig. S5), all samples show peaks corresponding to symmetric and asymmetric stretching vibrations of carboxylate groups (in cm^{-1}): **Eu-Dif** (ν_{as} = 1587(s), ν_s = 1362(s)), **Eu-St** (ν_{as} = 1595(s), ν_s =1358(s)), **Eu-M** (ν_{as} = 1588(s), ν_s = 1364(s)), **Tb-Dif** (ν_{as} = 1596(s), ν_s = 1360(s)), **Tb-St** (ν_{as} = 1589(s), ν_s = 1363(s)), **Tb-M** (ν_{as} = 1586(s), ν_s = 1362(s)). The samples also show a broad band in the region of 3700-3000 cm^{-1}, most likely corresponding to νOH due to the presence of coordinated and hydration water molecules. In some samples (**Eu-Dif**, **Tb-St**), a peak at 3133 cm^{-1} can be seen, corresponding to νNH vibrational mode. The FTIR spectra of the organic acids and their corresponding sodium salts are represented in the Fig. S6. Essentially, all samples exhibit the same vibrational modes, with some bands being better resolved in the more crystalline samples such as **Eu-St** and **Tb-St**, in good agreement with the PXRD data.

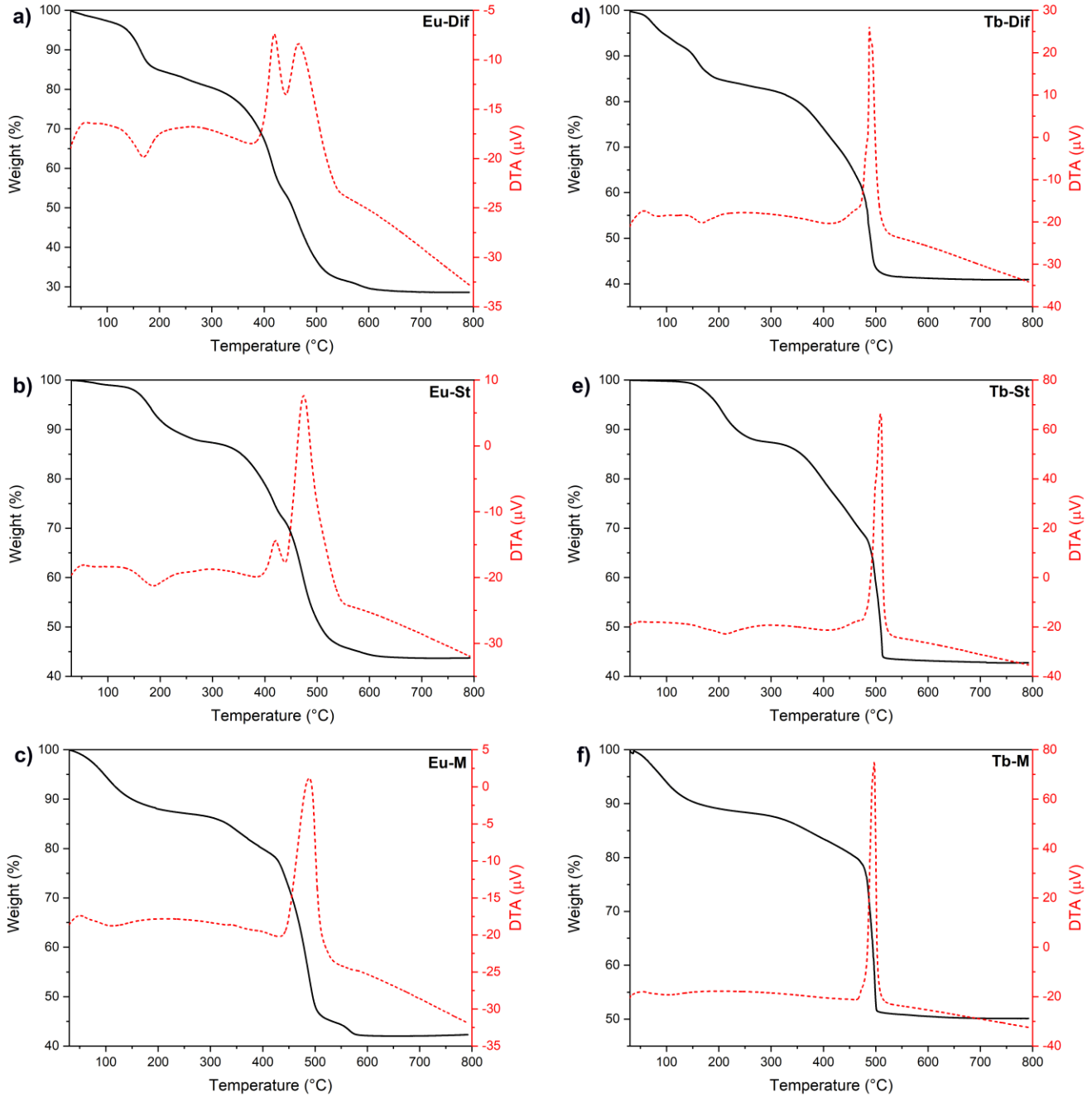

Fig. S7. TGA/DTA curve plots for **Eu-Dif** (a), **Eu-St** (b), **Eu-M** (c), **Tb-Dif** (d), **Tb-St** (e) and **Tb-M** (f).

Table S1. Thermal data of the samples.

Sample	T_{onset} (°C)	DTA endo peak (°C)	DTA exo peak (°C)
Eu-Dif	401.2	169.6	419.4 465.7
Eu-St	417.9	187.5	420.2 474.4
Eu-M	425.1	111.3	488.6
Tb-Dif	417.8	167.7	487.9
Tb-St	418.7	212.2	509.4
Tb-M	425.1	-	496.8

Thermogravimetric and Differential Thermal Analysis (TGA/DTA) of the samples after methanol-exchange activation process were carried out and the corresponding curves are shown in Fig. S7. The thermal stabilities of the compounds (calculated from the onset temperature) are similar, being approximately 410°C (see Table S1). For all samples, a weight loss of ca. 5% between 30-100°C indicates the solvent loss and ca. 20% (100-355°C) indicates the loss of coordinated water, with subsequently linker combustion and framework collapse. A thermal stability of ca. 410°C is on par with similar reported compounds.[1–3]

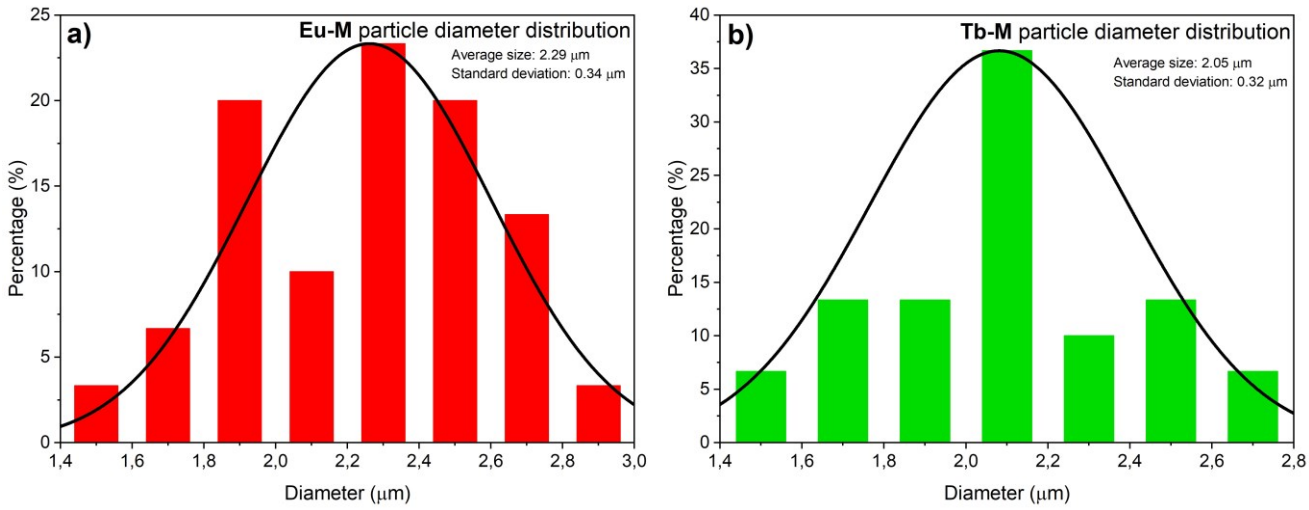

Fig. S8. Particle diameter distribution for **Eu-M** (a) and **Tb-M** (b) compounds.

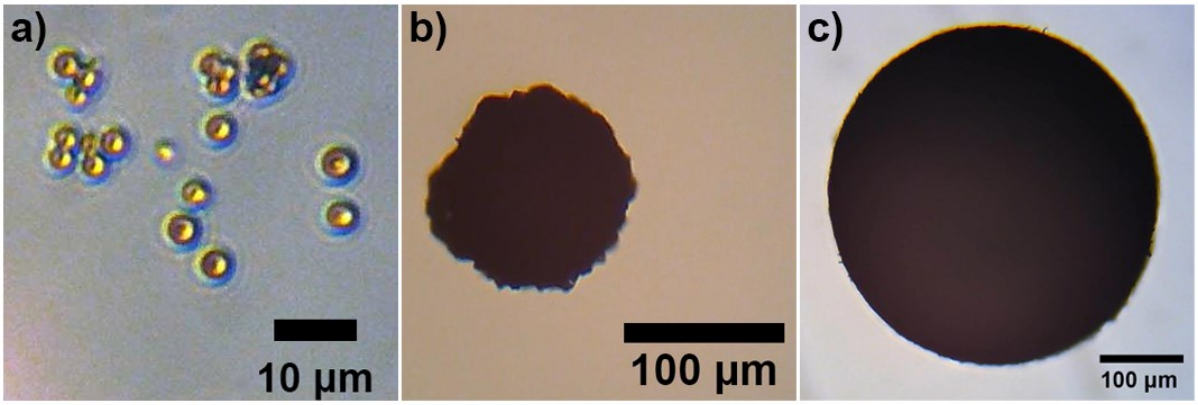

Fig. S9. Optical micrographs of **Tb-M** (a), **Tb-St** (b) and **Tb-Dif** (c).

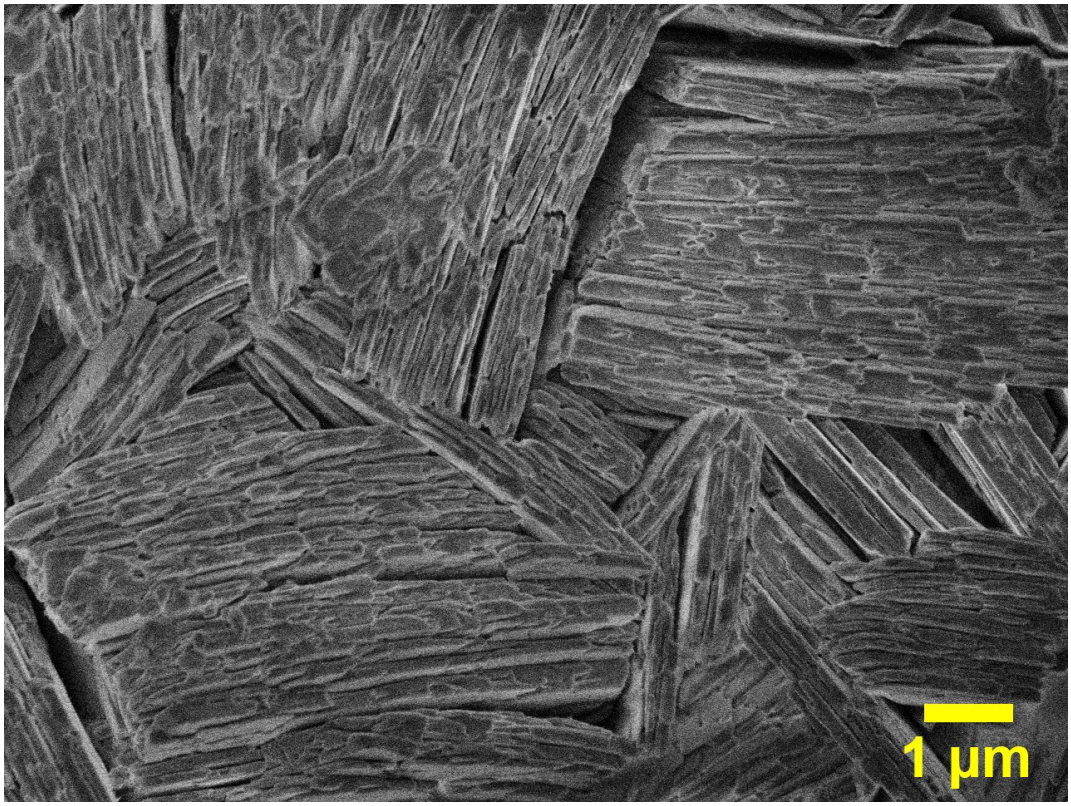

Fig. S10. SEM image showing a closer view on the surface of **Tb-Dif** sample.

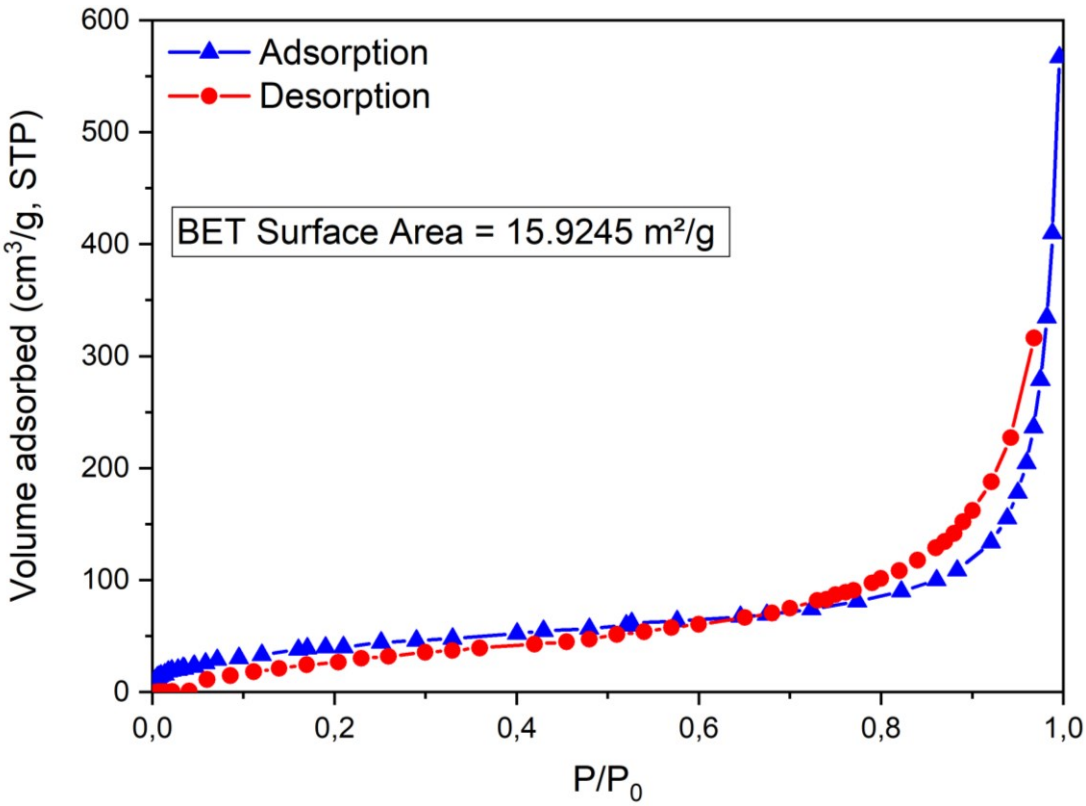

Fig. S11. N_2 adsorption/desorption isotherms for **Tb-M** sample exhibiting a behavior similar to non-porous solids. The calculated BET surface area is of 15.9245 m^2/g.

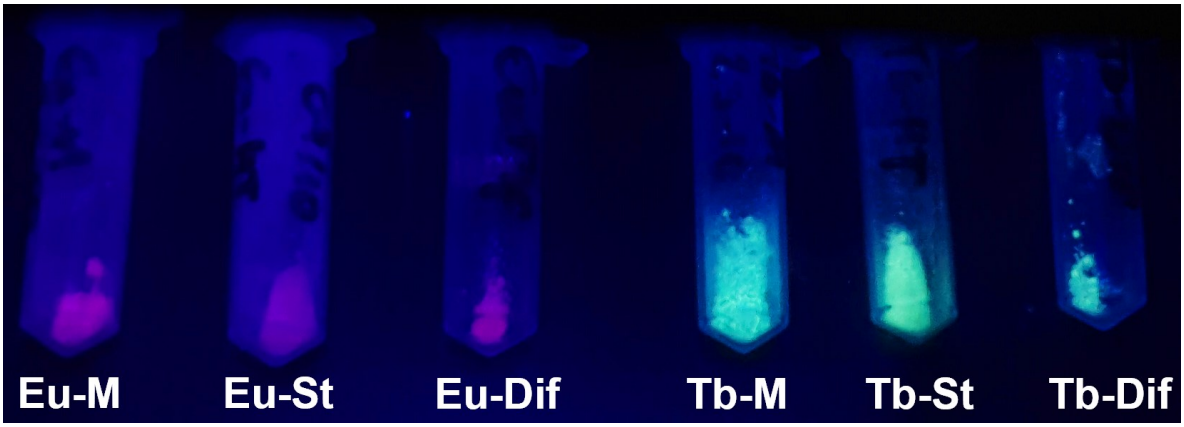

Fig. S12. Photograph of the samples under λ_{ex} = 365 nm UV light.

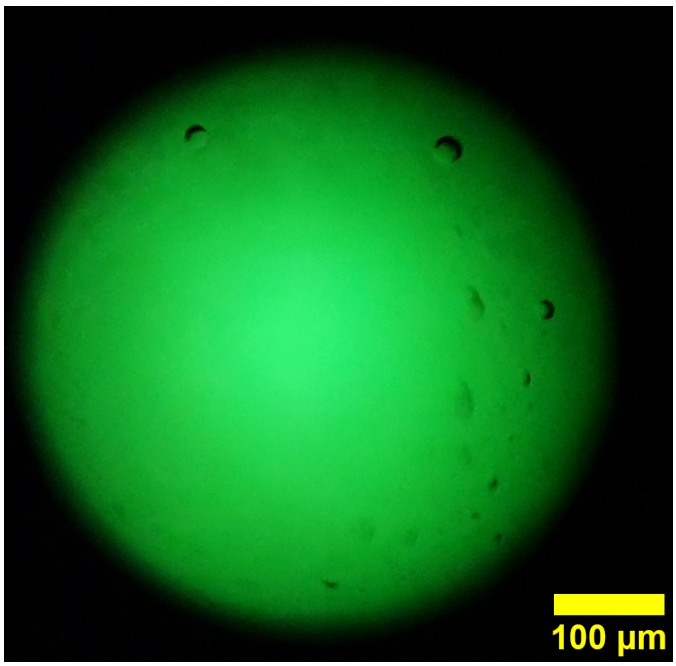

Fig. S13. Fluorescence micrograph of **Tb-Dif** sample under λ_{ex} = 358 nm UV light.

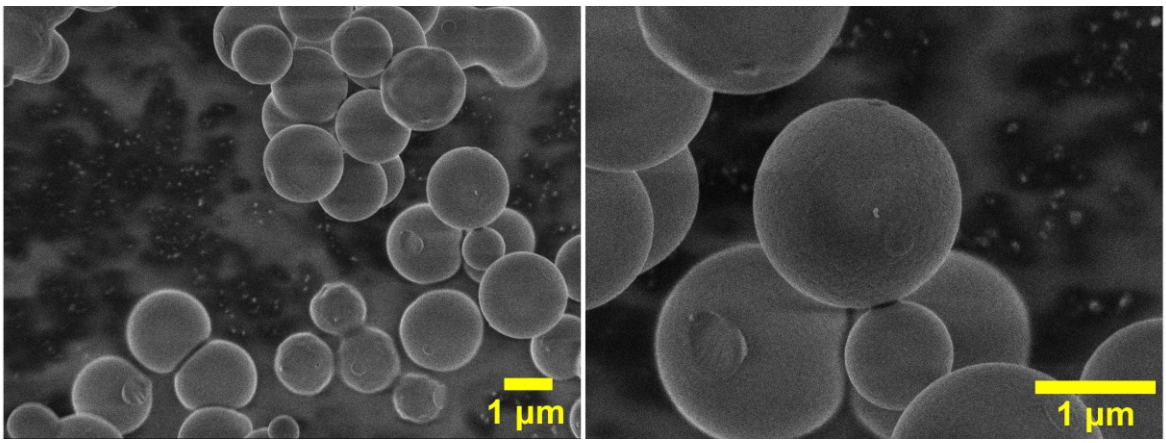

Fig. S14. FEG-SEM images of **Gd-M** sample.

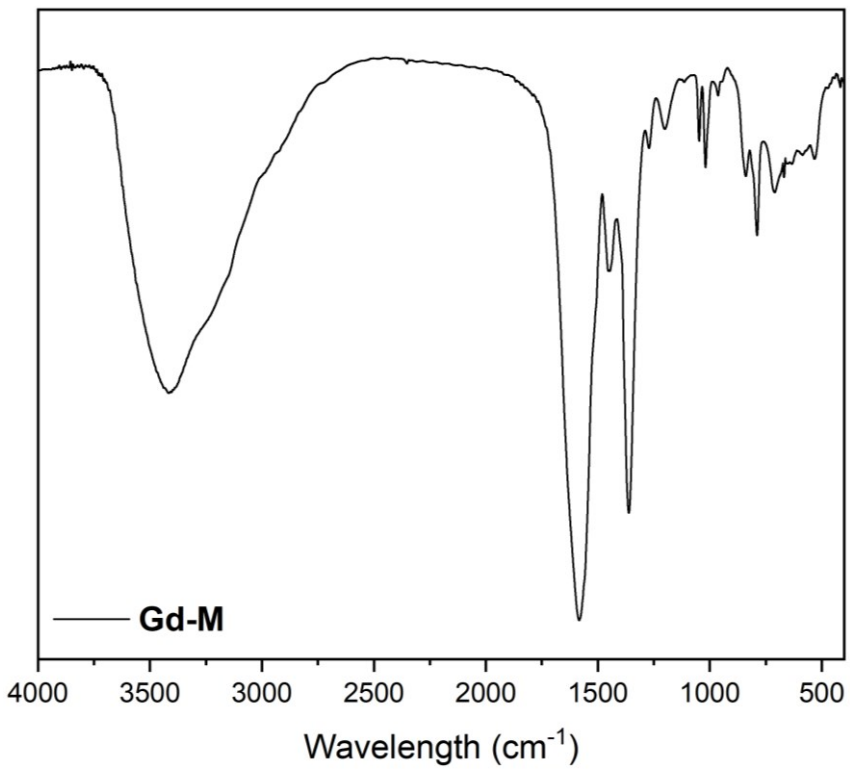

Fig. S15. FTIR spectrum of **Gd-M** sample.

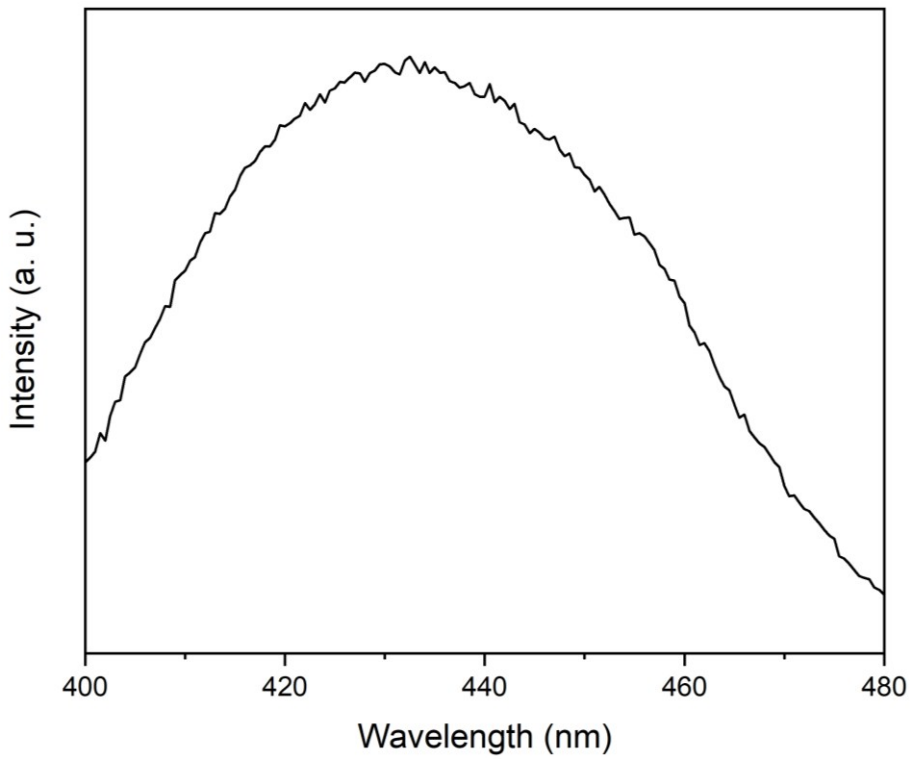

Fig. S16. Emission spectrum (λex = 272 nm) measured at 77 K for **Gd-M** sample.

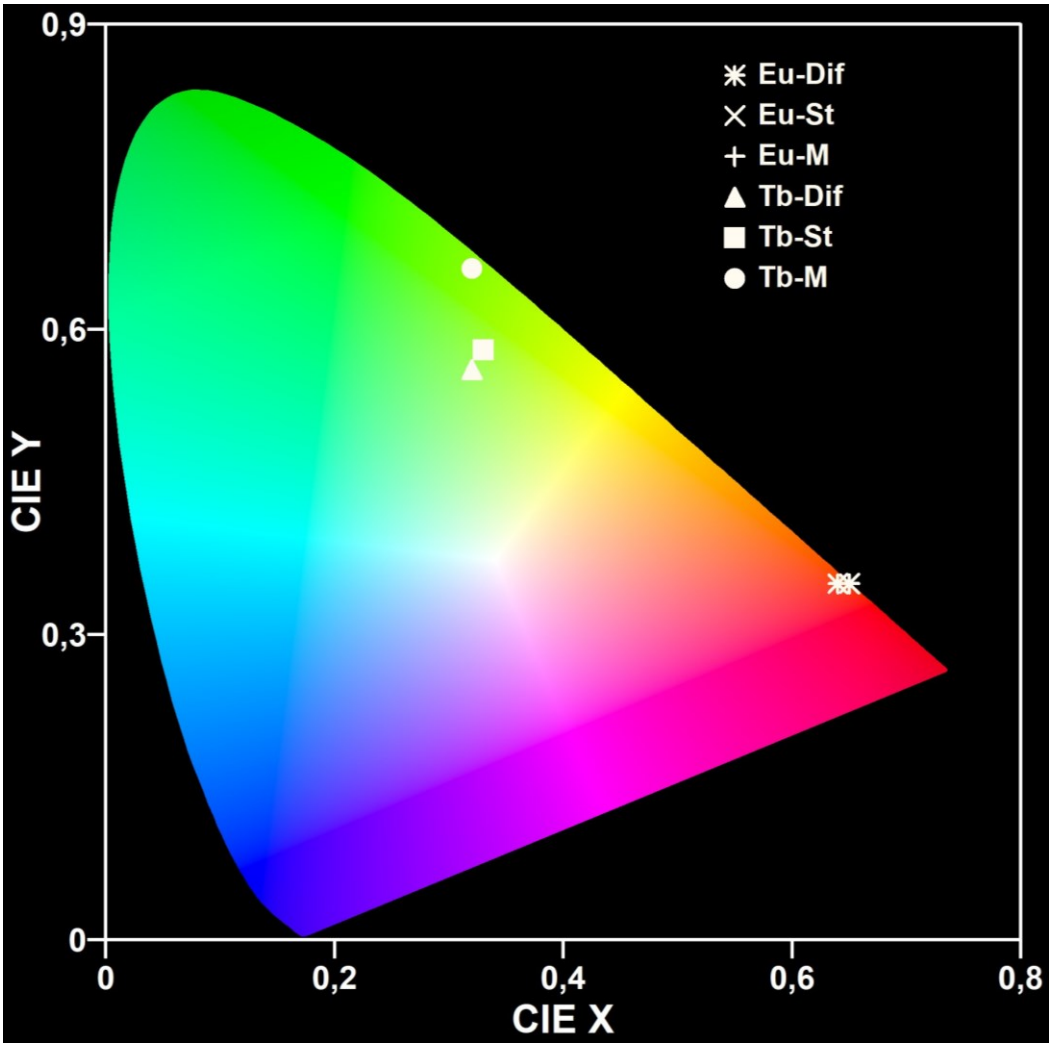

Fig. S17. CIE 1931 diagram exhibiting the points related to each coordinate for the samples.

Table S2. CIE 1931 coordinates (x, y) for each sample.

Sample	**Eu-Dif**	**Eu-St**	**Eu-M**	**Tb-Dif**	**Tb-St**	**Tb-M**
CIE coordinates	(0.67, 0.33)	(0.68, 0.32)	(0.68, 0.32)	(0.30, 0.53)	(0.30, 0.55)	(0.30, 0.66)

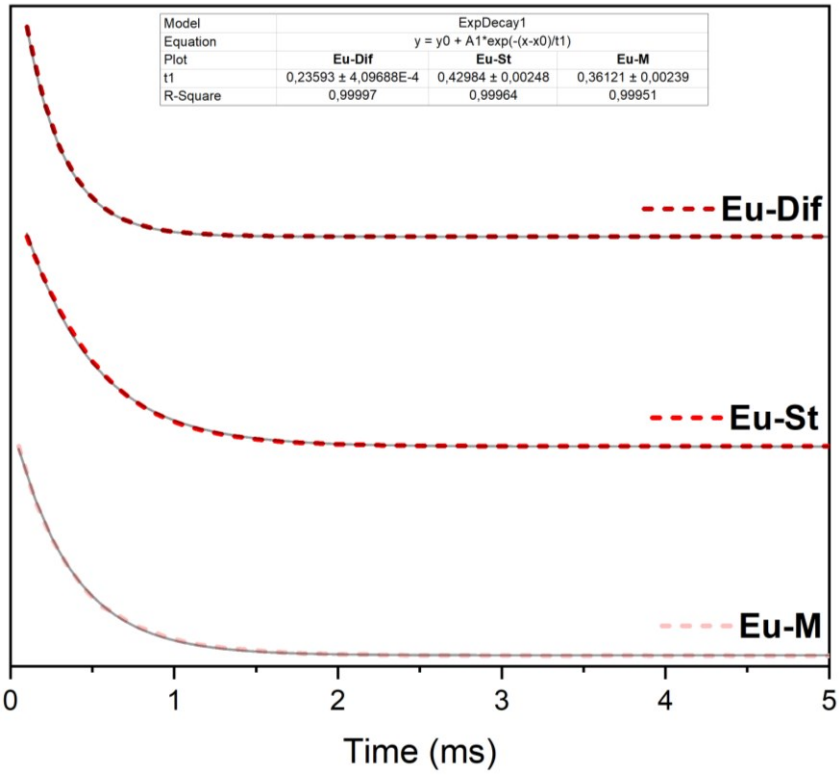

Fig. S18. Excited state decay curves for Eu^{3+}-based samples (dashed lines) and the fitted first-order exponential decay (full lines). Inset: Table showing the luminescence lifetime values and R-square.

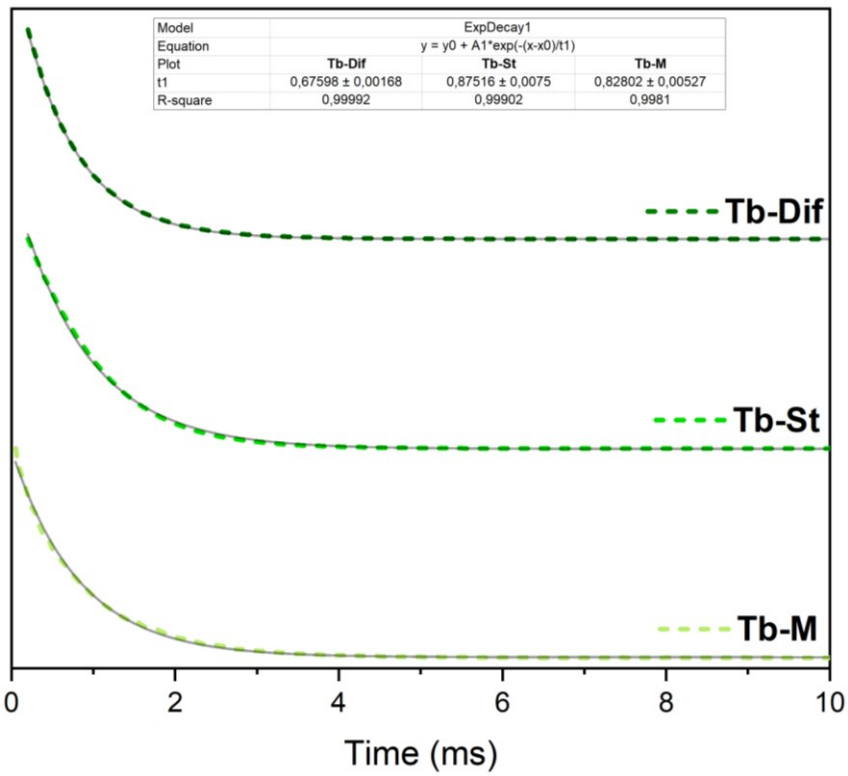

Fig. S19. Excited state decay curves for Tb^{3+}-based samples (dashed lines) and the fitted first-order exponential decay (full lines). Inset: Table showing the luminescence lifetime values and R-square.

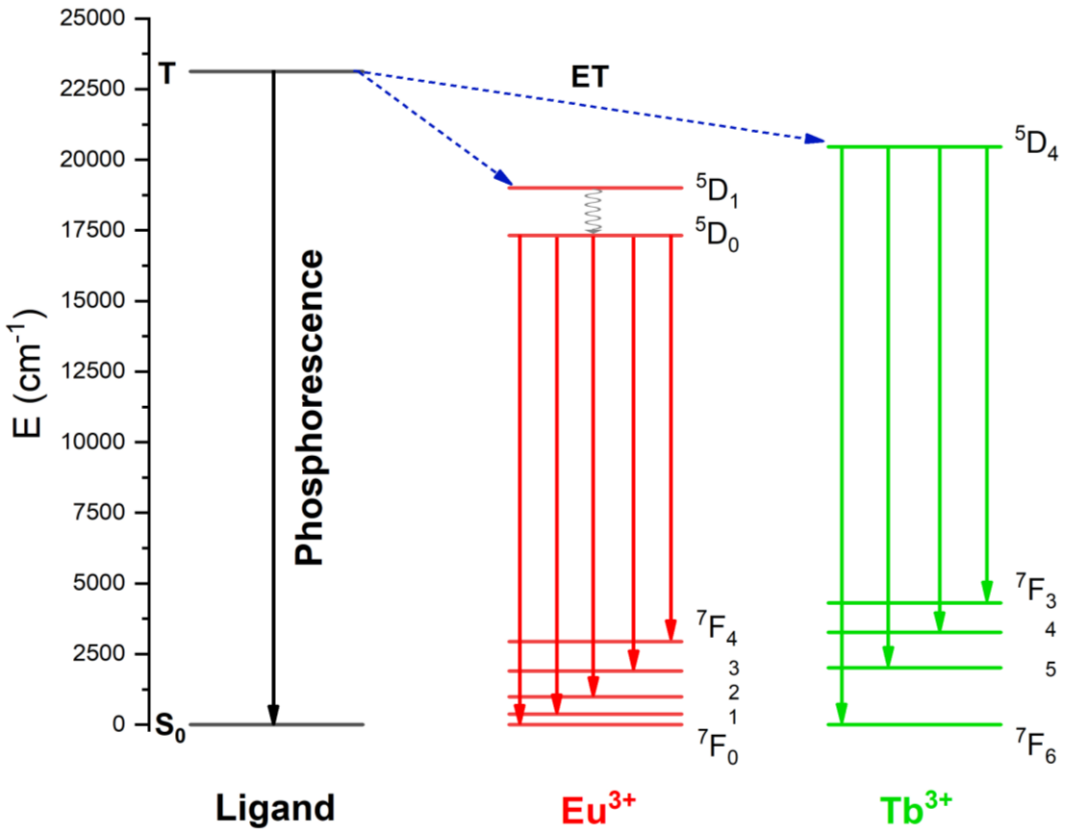

Fig. S20. Jablonski diagrams schematizing the triplet state (T) relaxation to ground state (S_0) in the ligand, the energy transfer processes (ET), other non-radiative processes (grey arrow) and main transitions in Eu^{3+} and Tb^{3+} which are visible in the emission spectra.

References

1 L. Pan, X.-Y. Huang, J. Li, Y.-G. Wu and N.-W. Zheng, *Angew. Chem. Int. Ed.*, 2000, **39**, 527-530.

2 H.-Y. Wu, S.-T. Yue, N. Wang and Y.-L. Liu, *J. Coord. Chem.*, 2010, **63**, 785–793.

3 T. Jing, L. Chen, F. Jiang, Y. Yang, K. Zhou, M. Yu, Z. Cao, S. Li and M. Hong, *Cryst. Growth Des.*, 2018, **18**, 2956–2963.